J Comput Aided Mol Des (2009) 23:845–852
DOI 10.1007/s10822-009-9301-4

Conformational analysis of thioglycoside derivatives of histo-blood group ABH antigens using an ab initio-derived reparameterization of MM4: implications for design of non-hydrolysable mimetics

Francesco Strino · Jenn-Huei Lii · Hans-Joachim Gabius · Per-Georg Nyholm

Received: 14 July 2009 / Accepted: 31 August 2009 / Published online: 15 September 2009

Abstract Histo-blood group ABH antigens serve as recognition sites for infectious microorganisms and tissue lectins in intercellular communication, e.g. in tumor progression. Thus, they are of interest as a starting point for drug design. In this respect, potent non-hydrolysable derivatives such as thioglycosides are of special interest. As prerequisite to enable estimations of ligand properties relative to their natural counterparts, conformational properties of the thioglycosidic derivatives of ABH trisaccharides and their disaccharide units were calculated using systematic and filtered systematic searches with the MM4 force field. Parameters for the glycosidic torsions of thioglycosides were independently derived from ab initio calculations. The resulting energy deviations required a reparameterization of MM4 to a new parameter set called MM4R. The data sets obtained using MM4R reveal that the thioglycosides have somewhat increased levels of flexibility about the major low-energy conformations shared with the corresponding O-glycosides. In the trisaccharides, the thiosubstitution of the Gal[NAc]α1-3Gal linkage leads to a preference for a conformation which is the secondary minimum of the natural counterparts. This conformation also generates contacts between the *N*-acetyl group and the fucose moiety in the blood group A derivative. Calculations further indicate that thiosubstitution of only the Fucα1-2Gal linkage does not affect the conformational preferences compared to the natural trisaccharide. Thiosubstitution of both linkages in the trisaccharide results in increased flexibility but the favored conformation of the natural trisaccharides is preferred. The study suggests that thioglycoside derivatives of ABH antigens could have pharmaceutical interest as ligands of lectins and other carbohydrate-binding proteins.

Keywords Blood group antigens · Drug design · Lectins · Molecular mechanics · Thioglycoside

F. Strino · P.-G. Nyholm (✉)
Institute of Biomedicine/Section of Medical Biochemistry, Göteborg University, Medicinaregatan 9, 40530 Göteborg, Sweden
e-mail: nyholm@medkem.gu.se; per-georg.nyholm@medkem.gu.se

J.-H. Lii
Department of Chemistry, National Changhua University of Education, Changhua 50058, Taiwan

H.-J. Gabius
Institut für Physiologische Chemie, Tierärztliche Fakultät, Ludwig-Maximilians-Universität München, Veterinärstr. 13, 80539 München, Germany

Introduction

The ABH family of histo-blood group antigens was originally defined in transfusion medicine, where incompatibility results in severe complications [1]. The search for reagents, which reliably distinguish between these epitopes on erythrocytes in clinical practice, prompted systematic screening of plant extracts. This work—together with applying the H-specific eel serum and sugars as inhibitors of lectin-dependent hemagglutination—led to the identification of the carbohydrate nature of the ABH blood group substances [2, 3]. Binding of these determinants by proteins is not limited to the mentioned laboratory tools and serum antibodies. Of medical relevance, bacteria and viruses as well as normal and tumor cells can bind to the tri- and tetrasaccharide determinants [4–7]. In lung cancer this interaction has prognostic relevance [8]. Evidently, these glycans are important bioactive ligands on the cell surface [9]. This

emerging functionality explains why they are becoming innovative targets for drug development, aimed at blocking the physiologic interaction with adhesins of infectious microorganisms, plant toxins and tissue lectins promoting e.g. tumor growth, progression and spread. Within this quest, thioglycosides attract attention as potential drug leads due to their stability against hydrolysis [10, 11].

S-glycosides can readily be produced either chemically [10, 12, 13] or enzymatically with glycoligases for thiosugars [11, 14], or by using dynamic combinatorial libraries for glycosyldisulfides [15]. Interestingly, lectin-binding properties for a plant toxin and adhesion/growth-regulatory galectins have recently been revealed for digalactosyldisulfide [15]. In this respect, it is an intriguing challenge to define any difference between O- and S-glycosides which can affect the ligand properties such as the preferentially adopted shape. ABH-positive glycoproteins are strongly reactive to the mentioned mammalian lectins and to bacterial adhesins [16–18]. Thus, non-hydrolysable derivatives, if equivalent biochemically as ligands, may become clinically useful inhibitors. This perspective explains the interest to thoroughly map their conformational space in comparison to that of the natural ABH determinants.

Only few earlier studies on conformational properties of thioglycosides [19–21] have been reported in the literature, none of them focusing on the S-forms of ABH determinants. Since suitable parameterization of a force field for thioglycosides was not available, we set out with ab initio calculations prior to MM4-based force field calculations.

Methods

Herein, the notation (1→*X*) indicates the natural O-glycosidic linkage and (1–S→*X*) a thioglycosidic linkage. Torsion angles are defined using the *heavy atom* definition. Exemplified for the (1–S→2) bond, the angles are φ = O5–C1–S–C'2 and ψ = C1–S–C'2–C'3. The notation BGA-*x*/*x* is used for the histo-blood group A epitope to specify the type of the glycosidic bond (*x* can be O for O-glycosidic or S for thioglycosidic) in the cases of α-D-Gal*p*NAc-(1→3)-β-D-Gal*p* and α-L-Fuc*p*-(1→2)-β-D-Gal*p* linkages, respectively. Histo-blood group B derivatives are similarly characterized using the BGB-*x*/*x* notation.

The conformational space of all compounds was initially investigated by filtered systematic search with the molecular mechanics MM3(96) program [22–24]. Missing parameters were inferred by MM3 using its parameter estimator [25]. The MM4(03) [26–29] program was also tested but results suffered from poor quality of parameters obtained by applying the MM4 parameter estimator for the C–O–C–S and O–C–S–C torsions and the O–S–C bending. To address this issue, the fragment CH_3–O–CH_2–S–CH_3 was considered for an ab initio parameterization with respect to rotational barriers and conformational equilibria. Four torsional potential profiles were investigated. These profiles were constructed by rotating C–O–C–S (while O–C–S–C was kept at 60° and 180°) and O–C–S–C (while C–O–C–S was kept at 60° and 180°) dihedral angles using a 30° interval. Quantum mechanical calculations using the Becke3LYP/6-311+G* DFT theory were carried out by using the Jaguar software (Schrödinger LLC, Portland, OR, USA). The Becke3LYP DFT theory was chosen instead of the MP2 because of computing-time consideration and concerns about the intramolecular basis set superposition errors (BSSE). According to Lii and Allinger's [30] carbohydrate study, Becke3LYP theory usually results in a smaller BSSE than MP2. Each conformer was minimized. Bond distances and angles were also sampled for each conformation. These rotational energy profiles were then combined for the optimization of MM4 torsional parameters. Two types of MM4 torsional parameters (C–O–C–S: type 1-6-1-15 and O–C–S–C: type 6-1-15-1) were optimized simultaneously using the least-squares fitting program TORSFIND, which requires an internally generated MM3/MM4 input and an experimental (or quantum mechanics) energy profile as input. The procedure allowed us to update all related torsional parameters at the same time whenever other parameters, such as O–C–S (type 6-1-15) bending, were changed. The MM4 force field with these new parameters is referred as MM4R. The calculations of the energy levels were done using the MM4R parameters and a dielectric constant of 80 to simulate an aqueous environment.

Systematic searches were initially performed on all disaccharide substructures in the AB-derivatives using a step size of 15° of the φ and ψ glycosidic torsion angles. The two energetically favored conformations of the C5–C6 bond were investigated for each residue. Clockwise (C) and anti-clockwise (R) arrangements of the secondary hydroxyl groups were also considered. The sampled points were then used to draw adiabatic energy maps. The established disaccharide maps served as filters for generating the trisaccharide maps. All conformations with a more than 12 kcal/mol energy difference from the relative global minimum of the disaccharide were rigorously excluded. This simple filtering allowed skipping actual energy assessment of 50–80% of sampled conformations. The population density of relative minima was estimated by first computing Boltzmann probabilities of each grid point at 25 °C and then summing up all data points within the 3 kcal/mol isocontour. Uninteresting regions of the conformational space with more than a 2 kcal/mol difference from the global minimum were excluded.

Adiabatic potential energy maps were then computed for all possible combinations of O- and S-linkages of the three pyranose rings. The four-dimensional maps (BGA-O/O,

BGA-S/O, BGA-O/S, BGA-S/S, BGB-O/O, BGB-S/O, BGB-O/S, and BGB-S/S) were set up with a step size of 15° for the torsion angles of the glycosidic linkages.

The GLYGAL [31, 32] software was applied for running the energy calculations, analyzing the obtained data, and drawing the adiabatic maps. The molecular graphics was realized with Sybyl 8.0 (Tripos Inc., St. Louis, MO, USA). Molecular surfaces were visualized by means of the MOLCAD module of Sybyl. The lipophilic potential was calculated using the small-molecule option provided by MOLCAD [33] with published parameterization [34].

Results and discussion

Ab initio on methoxy(methylthio)methane

The ab initio calculations on the fragment CH_3–O–CH_2–S–CH_3 yielded torsion energy profiles shown in Fig. 1. They are in fair agreement with previous studies [19, 35]. However, our profiles of the O–C–S–C torsion with C–O–C–S fixed at around 60°, important for calculation on α-thioglycosides in the present study, did not come up with a valley at 180°, characteristic for the PCILO calculations [19]. Of note, the calculated energy preference for +sc compared to the −sc conformation is less in the case of O–C–S–C than for the O–C–O–C torsion. In the torsional profile of O–C–S–C with the C–O–C–S fixed at 60° (Fig. 1) this difference is only 2 kcal/mol, whereas it is 4 kcal/mol in the O–C–O–C [27] profile.

The deviations between the ab initio results and the corresponding force field results with MM4 were significant. Therefore, MM4 was reparametrized based on the present results, and we denoted the new parameter set MM4R (Table 1). Good agreement with the ab initio calculations was achieved (Fig. 1), and the MM4R was thus used in following calculations.

Disaccharide derivatives

The results of the systematic search of the disaccharides are summarized in Table 2 and the adiabatic maps are shown in Fig. 2.

The disaccharide α-L-Fuc*p*-(1→2)-β-D-Gal*p*, common to all ABH antigens, has a global minimum at $\varphi/\psi \approx -90°/-120°$ (Fig. 2a). Its secondary minimum at $\varphi/\psi \approx -90°/45°$ resides more than 2 kcal/mol higher than the global minimum. The impact of S-substitutions was studied next. The α-L-Fuc*p*-(1–S→2)-β-D-Gal*p* (Fig. 2a') shows a much broader low-energy region around the global minimum. The secondary minimum is also spatially more extended than for the O-glycoside, and the relative energy difference is negligible. The extent of population residing in the low-energy region corresponding to the global minimum of the O-glycoside is around 60%, while the second region accounts for about 35% of the population.

The map for the α-D-Gal*p*NAc-(1→3)-β-D-Gal*p* disaccharide of the histo-blood group A epitope (Fig. 2b) shows a well-defined global minimum at $\varphi/\psi \approx 75°/90°$, but other values of the ψ angle are also accessible. The

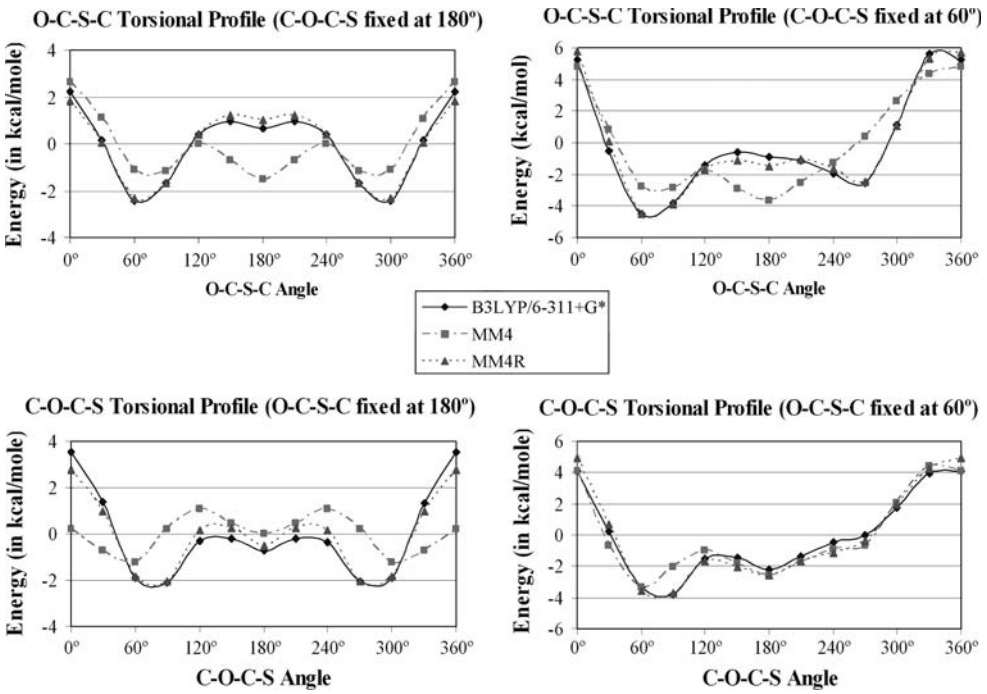

Fig. 1 Profiles for the torsion angles of the fragment CH_3–O–CH_2–S–CH_3. In the graphs the torsional profiles calculated with the standard MM4 force field, MM4 with the new parameter set (MM4R), and the B3LYP/6-311+G* theory are shown (see *central inset* for assignment of curves)

Table 1 The MM4R torsional parameters for C–O–C–S and O–C–S–C and the bending parameters for O–C–S

Torsional	T1[a]	T2[a]	T3[a]	T4[a]	V1[b]	V2[b]	V3[b]	V4[b]	V6[b]
COCS	1	6	1	15	−0.017	−3.2159	0.762	0.225	−0.033
OCSC	6	1	15	1	−1.476	−1.389	0.495	0.224	−0.003
Bending	T1[a]	T2[a]	T3[a]		K_b^c	θ^{od}			
O–C–S	6	1	15		0.695	108.5			

[a] MM4 atom types

[b] kcal/mol

[c] mdyne Å rad^{-2}

[d] Degrees

Table 2 Description of the energetically favorable conformations of the disaccharide moieties of histo-blood group antigens and their thioglycosidic derivatives

Linkage	φ/ψ	Energy (kcal/mol)	Population (%)
α-L-Fuc*p*-(1→2)-β-D-Gal*p*	−90°/−120°		99.0
α-L-Fuc*p*-(1–S→2)-β-D-Gal*p*	−90°/−90°		62.4
	−90°/45°	+ 0.03	35.1
α-D-Gal*p*NAc-(1→3)-β-D-Gal*p*	75°/90°		93.4
α-D-Gal*p*NAc-(1–S→3)-β-D-Gal*p*	75°/60°		77.3
	75°/−75°	+ 0.40	14.8
α-D-Gal*p*-(1→3)-β-D-Gal*p*	75°/90°		93.4
α-D-Gal*p*-(1–S→3)-β-D-Gal*p*	90°/75°		75.4
	75°/−60°	+ 0.43	19.2

thiodiglycoside α-D-Gal*p*NAc-(1–S→3)-β-D-Gal*p* (Fig. 2b') has the same preferred conformations but an elevated degree of flexibility of the φ angle. The secondary minimum at 75°/−60° becomes energetically favorable (only +0.4 kcal/mol from the global minimum) and accounts for 15% of the total population, while the low-energy area around the global minimum accounts for around 75%. The presence of a second conformational family in a related thiodisaccharide derivative has been previously calculated and verified for the disaccharide α-L-Fuc*p*-(1–S→3)-α-D-Gal*p*NAc [20]. The α-D-Gal*p*-(1–*X*→3)-β-D-Gal*p* disaccharides (Fig. 2c, c') showed properties very similar to their GalNAcα1-3 Gal counterparts.

Furthermore, it can be noted that the secondary positions for the φ angle ($\varphi/\psi \approx 90°/-120°$ Fig. 2a, a' and $\varphi/\psi \approx -90°/120°$ Fig. 2b, b') become more favorable for the thioglycosides. This effect can be explained by the presence of an energy valley at −90° in the O–C–S–C torsional profile (Fig. 1).

Trisaccharide derivatives

Having completed the analysis of the disaccharide constituents, the description of the conformational properties of S-substituted trisaccharides with a branch point at the central galactose moiety was the next issue to be addressed. Spatial vicinity between sugars may cause alterations in

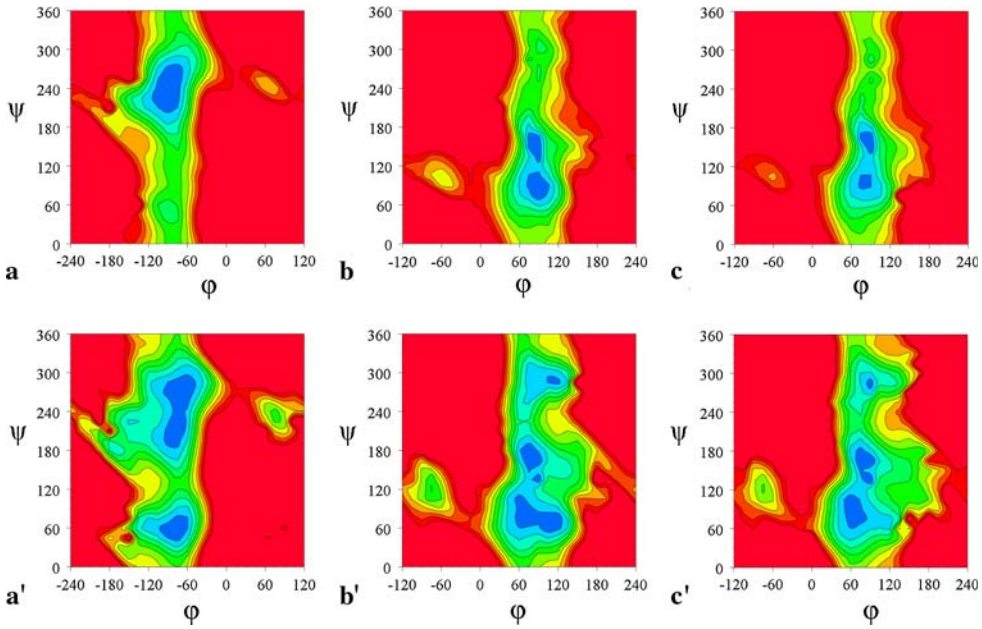

Fig. 2 Adiabatic maps for the disaccharide unit of the ABH histo-blood group antigens. Contour levels are drawn at steps of 1 kcal/mol with high- to low-energy regions colored from *red* to *blue* gradually. **a** α-L-Fuc*p*-(1→2)-β-D-Gal*p*; **a'** α-L-Fuc*p*-(1–S→2)-β-D-Gal*p*; **b** α-D-Gal*p*NAc-(1→3)-β-D-Gal*p*; **b'** α-D-Gal*p*NAc-(1–S→3)-β-D-Gal*p*; **c** α-D-Gal*p*-(1→3)-β-D-Gal*p*; **c'** α-D-Gal*p*-(1–S→3)-β-D-Gal*p*

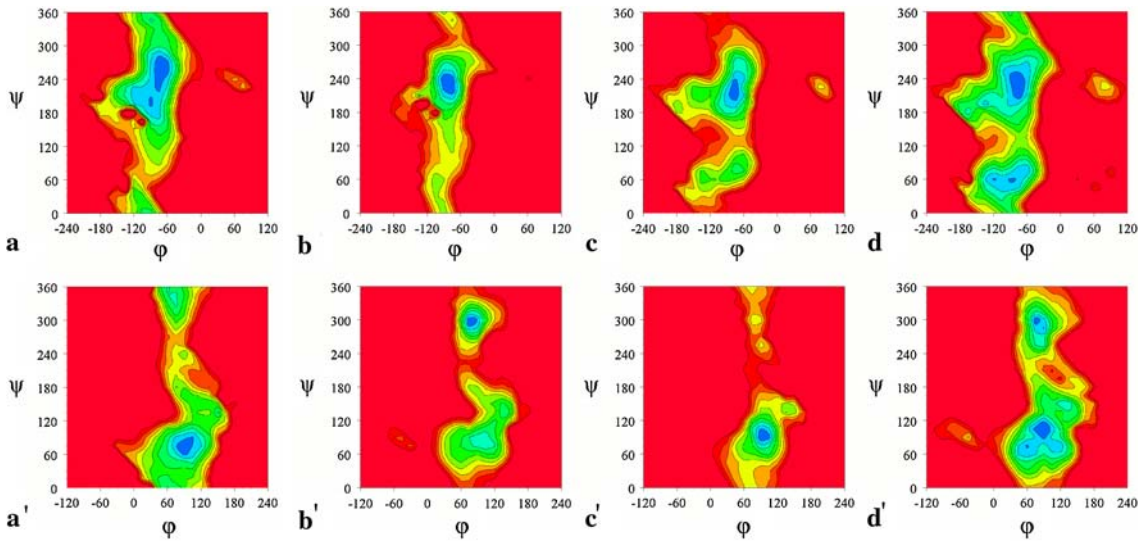

Fig. 3 Adiabatic maps for the glycosidic linkages in the histo-blood group A-trisaccharide and its thioglycosidic derivatives. **a** BGA-O/O α-L-Fuc*p*-(1→2)-*β*-D-Gal*p*; **a'** BGA-O/O α-D-Gal*p*NAc-(1→3)-*β*-D-Gal*p*; **b** BGA-O/S α-L-Fuc*p*-(1→2)-*β*-D-Gal*p*; **b'** BGA-O/S α-D-Gal*p*NAc-(1–S→3)-*β*-D-Gal*p*; **c** BGA-S/O α-L-Fuc*p*-(1–S→2)-*β*-D-Gal*p*; **c'** BGA-S/O α-D-Gal*p*NAc-(1→3)-*β*-D-Gal*p*; **d** BGA-S/S α-L-Fuc*p*-(1–S→2)-*β*-D-Gal*p*; **d'** BGA-S/S α-D-Gal*p*NAc-(1–S→3)-*β*-D-Gal*p*

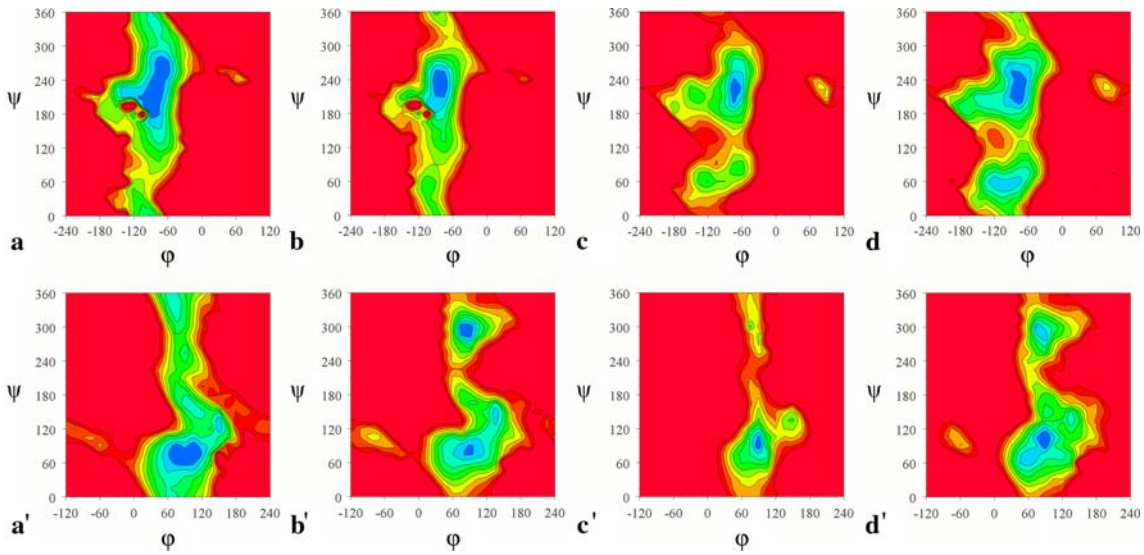

Fig. 4 Adiabatic maps for the glycosidic linkages in the histo-blood group B-trisaccharide and its thioglycosidic derivatives. **a** BGB-O/O α-L-Fuc*p*-(1→2)-*β*-D-Gal*p*; **a'** BGB-O/O α-D-Gal*p*-(1→3)-*β*-D-Gal*p*; **b** BGB-O/S α-L-Fuc*p*-(1→2)-*β*-D-Gal*p*; **b'** BGB-O/S α-D-Gal*p*-(1–S→3)-*β*-D-Gal*p*; **c** BGB-S/O α-L-Fuc*p*-(1–S→2)-*β*-D-Gal*p*; **c'** BGB-S/O α-D-Gal*p*-(1→3)-*β*-D-Gal*p*; **d** BGB-S/S α-L-Fuc*p*-(1–S→2)-*β*-D-Gal*p*; **d'** BGB-S/S α-D-Gal*p*-(1–S→3)-*β*-D-Gal*p*

conformational characteristics. However, the adiabatic maps for the glycosidic linkages of the O-glycoside for the histo-blood group A (Fig. 3a, a') and B epitopes (Fig. 4a, a') show similar conformational properties compared to those calculated for the disaccharides. Secondary conformations are restricted due to the vicinal branching. The calculations reveal a single well-defined conformation readily reconciled with previous studies [36] and available crystal structures such as PDB 2W7Y, 2VNG, 2O2L, and 2J1U. Next, energy maps were calculated for derivatives with at least one O→S substitution. The respective data sets are summarized in Table 3 and the adiabatic maps are shown in Figs. 3 and 4.

The α-L-Fuc*p*-(1–*X*→2)-*β*-D-Gal*p* linkages of the trisaccharides BGA-O/S (Fig. 3b), BGA-S/O (Fig. 3c), BGA-S/S (Fig. 3d), BGB-O/S (Fig. 4b), BGB-S/O (Fig. 4c), and

Table 3 Description of the energetically favorable conformations of histo-blood group antigens and their thioglycosidic derivatives

Compound	α-L-Fuc*p*-(1–*X*→2)-*β*-D-Gal*p*	α-D-Gal*p*NAc-(1–*X*→3)-*β*-D-Gal*p*	Energy (kcal/mol)	Population (%)
BGA-O/O	−75°/−105°	90°/75°		90.9
BGA-O/S	−90°/−120°	75°/−60°		89.0
	−90°/−120°	105°/75°	+2.38	3.7
BGA-S/O	−75°/−135°	90°/90°		94.0
BGA-S/S	−75°/−135°	90°/105°		42.3
	−75°/−120°	75°/−60°	+0.31	19.6
	−120°/60°	60°/75°	+0.86	12.8
	−90°/60°	75°/−60°	+0.91	13.0
BGB-O/O	−75°/−105°	90°/75°		91.4
	−135°/−150°	150°/135°	+1.24	1.6
BGB-O/S	−75°/−135°	75°/−60°		60.4
	−75°/−120°	90°/75°	+0.82	33.3
BGB-S/O	−75°/−135°	90°/90°		90.4
BGB-S/S	−75°/−135°	90°/105°		53.4
	−90°/−105°	75°/−60°	+0.91	21.9
	−120°/60°	60°/75°	+1.16	6.9
	−90°/60°	75°/−60°	+1.55	4.4

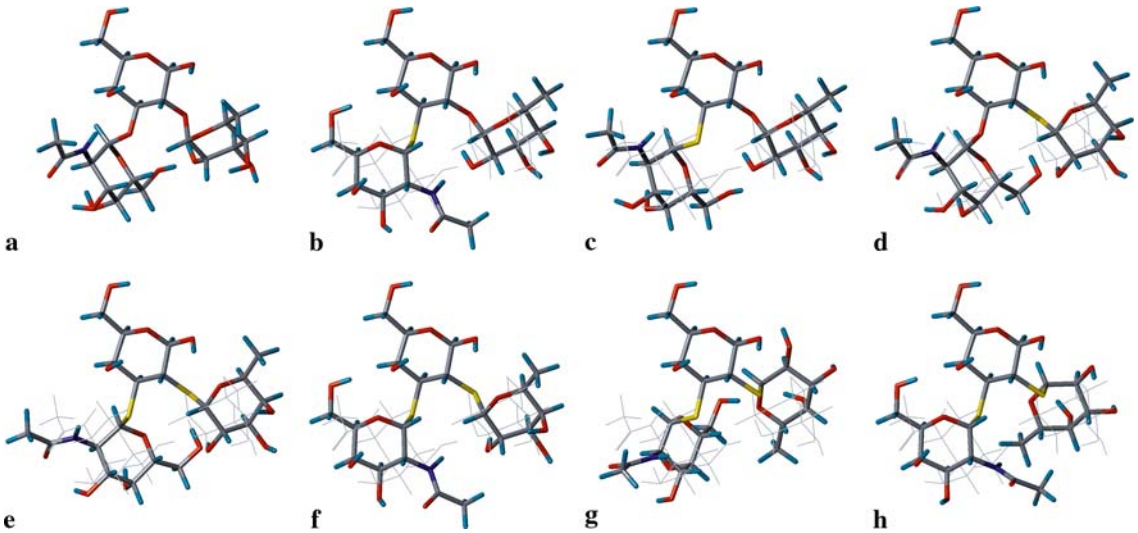

Fig. 5 Superimpositions on the Gal moiety of the energetically most favorable conformation of histo-blood group A (*BGA*) trisaccharide and its thioderivatives. The preferred conformation of the natural BGA is shown in *gray lines*. Multiple conformers are sorted by energy, where the global minimum is first. **a** BGA-O/O; **b** and **c** BGA-O/S; **d** BGA-S/O; **e**–**h** BGA-S/S

BGB-S/S (Fig. 4d), respectively, all share conformational properties with that of the respective O- and S- linked disaccharides. The secondary conformation is not significant in the S/O derivatives, while it accounts for 26% of the BGA-S/S and 11% of BGB-S/S.

The α1-3 extension of the galactose core behaves in a different manner. The thioderivatives can assume a secondary conformation for the α-D-Gal*p*NAc-(1–S→3)-*β*-D-Gal*p* moiety at $\varphi/\psi \approx 75°/-60°$. The α-D-Gal*p*NAc-(1–S→3)-*β*-D-Gal*p* linkage in O/S derivatives (Figs. 3b', 4b') strongly favors this conformation. Interestingly, in BGA-O/S the interaction between the *N*-acetyl group and the fucose moiety in this conformation makes it relatively more favorable than in the BGB-O/S, in proportions of 60:33 for the B-type compound and 89:4 for the A-trisaccharide.

The fully thiosubstituted BGA-S/S (Fig. 3d, d') and BGB-S/S (Fig. 4d, d') derivatives can access all four combinations of conformations for the two linkages with preference to the global minimum of their constituent disaccharide moieties.

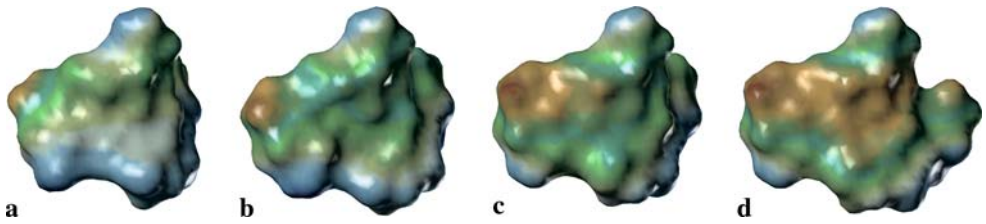

Fig. 6 Solvent-accessible surface of the histo-blood group A-trisaccharide BGA-O/O (**a**) and its derivatives BGA-O/S (**b**), BGA-S/O (**c**), and BGA-S/S (**d**) colored according to degree of lipophilicity (*blue*: hydrophilic, *brown*: lipophilic, *green*: intermediate). The structures are superimposed on the Gal moiety, and the compounds are oriented with the Fuc residue on the *left* and the Gal on the *right* to highlight the difference in lipophilic potential of the linkage atoms

The conformations of the BGA compounds are shown in Fig. 5. As expected, the BGB derivatives show very similar properties to their BGA counterparts, with the exception of the BGA-O/S derivative, where the *N*-acetyl group is involved in intramolecular interactions (Fig. 5b).

Other structural properties

Beside the conformation of the glycosidic linkages, the introduction of sulfur atoms also affects other factors relevant for receptor binding. Because the C–S bond is longer than the C–O bond, the ring distance in O-linked pyranoses is about 2.4 Å compared to 2.9 Å in thioglycosides. Furthermore, S-substitutions increase the hydrophobicity of the compound considerably as illustrated in Fig. 6. All compounds present a hydrophobic area around the methyl group of the fucose unit, whereas thioglycosides also show a hydrophobic patch in proximity of the sulfur atom(s).

Conclusions

The present results indicate in general an increase in flexibility upon S-substitutions. Thiosubstitution of the α-L-Fuc*p*-(1→2)-*β*-D-Gal*p* linkage has a minimal effect. However, the conformational properties of the α-D-Gal*p*-NAc-(1→3)-*β*-D-Gal*p* linkage are affected to a considerable extent. For the trisaccharides BGA-S/O and BGB-S/O, the calculations reveal a single conformation that mimics the natural compound.

The present study suggests that thioglycosides may have peculiar conformational properties which differ from those of their natural counterparts. Together with increased length of the glycosidic bond and hydrophobicity, this can have effects on bioactivity. However, certain partially thiosubstituted glycosides appear to have conformational properties very similar to those of their parent saccharides. Thus, MM4-based calculations, teamed up with docking, should lead to valuable predictions prior to synthetic work, It is expected that appropriately designed thioglycosides may offer a pharmaceutical potential as inhibitors and as tools in investigating interactions with lectins, aiding efforts to delineate mechanisms of ligand binding and lectin functionality [37].

Acknowledgments Financial support from the Swedish Medical Research Council (K2000-03x-00006-36A), the research initiative LMU*excellent,* an EC Marie Curie Research Training Network grant (MRTN-CT-2005-019561) and Biognos AB (Göteborg) is gratefully acknowledged. Also, access to the Linux cluster at the Institute of Biomedicine, Gothenburg University, Sweden is gratefully acknowledged.

References

1. Landsteiner K (1900) Zbl Bakt 27:357
2. Kilpatrick DC, Green C (1992) Adv Lectin Res 5:51
3. Watkins WM (1999) Trends Glycosci Glycotechnol 11:391
4. Reuter G, Gabius H-J (1999) Cell Mol Life Sci 55:368
5. Gabius H-J, Siebert H-C, André S, Jiménez-Barbero J, Rüdiger H (2004) Chembiochem 5:740
6. Le Pendu J (2004) Adv Exp Med Biol 554:135
7. Gabius H-J (2006) Crit Rev Immunol 26:43
8. Kayser K, Bovin NV, Korchagina EY, Zeilinger C, Zeng FY, Gabius H-J (1994) Eur J Cancer 30A:653
9. Gabius H-J (2008) Biochem Soc Trans 36:1491
10. Witczak ZJ (1999) Curr Med Chem 6:165
11. Jahn M, Marles J, Warren RAJ, Withers SG (2003) Angew Chem Int Ed Engl 42:352
12. Rye CS, Withers SG (2004) Carbohydr Res 339:699
13. Szilágyi L, Varela O (2006) Curr Org Chem 10:1745
14. Kim Y-W, Lovering AL, Chen H, Kantner T, McIntosh LP, Strynadka NCJ, Withers SG (2006) J Am Chem Soc 128:2202
15. André S, Pei Z, Siebert H-C, Ramström O, Gabius H-J (2006) Bioorg Med Chem 14:6314
16. Wu AM, Wu JH, Liu J-H, Singh T, André S, Kaltner H, Gabius H-J (2004) Biochimie 86:317
17. Wu AM, Singh T, Wu JH, Lensch M, André S, Gabius H-J (2006) Glycobiology 16:524
18. Imberty A, Varrot A (2008) Curr Opin Struct Biol 18:567
19. Tvaroska I (1984) Collect Czech Chem Commun 49:345
20. Aguilera B, Jiménez-Barbero J, Fernández-Mayoralas A (1998) Carbohydr Res 308:19
21. Mazeau K, Tvaroska I (1992) Carbohydr Res 225:27
22. Allinger NL, Yuh YH, Lii J-H (1989) J Am Chem Soc 111:8551
23. Allinger NL, Rahman M, Lii J-H (1990) J Am Chem Soc 112:8293
24. Lii J-H, Allinger NL (1991) J Comput Chem 12:186
25. Allinger NL, Zhou X, Bergsma J (1994) J Mol Struct 312:69

26. Allinger NL, Chen K-H, Lii J-H, Durkin KA (2003) J Comput Chem 24:1447
27. Lii J-H, Chen K-H, Durkin KA, Allinger NL (2003) J Comput Chem 24:1473
28. Lii J-H, Chen K-H, Grindley TB, Allinger NL (2003) J Comput Chem 24:1490
29. Lii J-H, Chen K-H, Allinger NL (2003) J Comput Chem 24:1504
30. Lii J-H, Ma B, Allinger NL (1999) J Comput Chem 20:1593
31. Nahmany A, Strino F, Rosen J, Kemp GJL, Nyholm P-G (2005) Carbohydr Res 340:1059
32. Strino F, Nahmany A, Rosen J, Kemp GJL, Sá-correia I, Nyholm P-G (2005) Carbohydr Res 340:1019
33. Heiden W, Moeckel G, Brickmann J (1993) J Comput Aided Mol Des 7:503
34. Ghose AK, Viswanadhan VN, Wendoloski JJ (1998) J Phys Chem A 102:3762
35. Matsuura H, Murata H (1983) J Mol Struct 96:267
36. Azurmendi HF, Bush CA (2002) Carbohydr Res 337:905
37. Gabius H-J (ed) (2009) The sugar code: fundamentals of glycosciences. Wiley–VCH, Wenheim